Methods and Applications

Nowcasting and Forecasting Seasonal Influenza Epidemics — China, 2022–2023

Zhanwei Du[1,2]; Zengyang Shao[2]; Xiao Zhang[2]; Ruohan Chen[2]; Tianmu Chen[3]; Yuan Bai[1,2]; Lin Wang[4]; Eric H. Y. Lau[5]; Benjamin J. Cowling[1,2,#]

ABSTRACT

Background: Seasonal influenza resurged in China in February 2023, causing a large number of hospitalizations. While influenza epidemics occurred across China during the coronavirus disease 2019 (COVID-19) pandemic, the relaxation of COVID-19 containment measures in December 2022 may have contributed to the spread of acute respiratory infections in winter 2022/2023.

Methods: Using a mathematical model incorporating influenza activity as measured by influenza-like illness (ILI) data for northern and southern regions of China, we reconstructed the seasonal influenza incidence from October 2015 to September 2019 before the COVID-19 pandemic. Using this trained model, we predicted influenza activities in northern and southern China from March to September 2023.

Results: We estimated the effective reproduction number R_e as 1.08 [95% confidence interval (*CI*): 0.51, 1.65] in northern China and 1.10 (95% *CI*: 0.55, 1.67) in southern China at the start of the 2022–2023 influenza season. We estimated the infection attack rate of this influenza wave as 18.51% (95% *CI*: 0.00%, 37.78%) in northern China and 28.30% (95% *CI*: 14.77%, 41.82%) in southern China.

Conclusions: The 2023 spring wave of seasonal influenza in China spread until July 2023 and infected a substantial number of people.

INTRODUCTION

In China, influenza virus exhibited apparent seasonality before the coronavirus disease 2019 (COVID-19) pandemic but was suppressed by multifaceted control strategies during the COVID-19 pandemic (*1*). However, due to the substantially reduced pathogenicity of the new COVID-19 variants, officials decided to adjust the response strategies (e.g., restricting testing coverage, shortening quarantine periods for inbound travelers, and suspending secondary contact tracing) to better balance public health and economic factors starting on November 11, 2022 (*2*); then, on December 7, 2022, control measures (e.g., the prohibition of regional mass testing and the implementation of home isolation or quarantine) were further relaxed (*3*).

During the COVID-19 pandemic, nonpharmaceutical interventions (NPIs) such as social distancing, school closures, bans on large gatherings and nonessential activities, stay-at-home orders, travel restrictions, wearing face masks, extensive testing, contact tracing, and isolation programs have all been successful in slowing the spread of the virus that causes COVID-19, thereby minimizing outbreaks and saving lives (*4*–*7*). In early 2020, NPIs were estimated to have reduced influenza activity in southern and northern China by 79.2% and 79.4%, respectively, in contrast with normal seasonal influenza activity (*8*). This outcome was undoubtedly positive, especially in the short term, as it reduced the spread of the virus and thus the number of infections. However, the reduced circulation of influenza may have negative consequences in the long term; for example, when fewer people have developed immunity to influenza, a population can be rendered slightly more vulnerable to infection in the following season (*9*–*10*).

In China, the national influenza vaccination coverage rate per year was particularly lower than that in other countries, at approximately 2.2% in 2014 (*11*), in contrast with 6.9% at the global scale (*12*). The lack of immune stimulation due to reduced circulation of influenza could result in a more severe outbreak in the following season, potentially leading to more hospitalizations and deaths (*10*). It is thus unsurprising that there was a large resurgence of influenza B and influenza A activity in China in July 2021 and June 2022 in Shanghai, respectively (*1*).

The eventual cancellation of COVID-19-related

NPIs (e.g., the prohibition of regional mass testing and the implementation of home isolation or quarantine) in China on December 7, 2022 (*3*) led to an unprecedentedly large Omicron wave in December 2022 together with a sharp increase in influenza incidence in February 2023 (*13*). As of March 12, 2023, 807 outbreaks had been detected in China (*14*). For improving the surveillance and early warning systems for influenza epidemics, in this study, we projected the influenza incidence and quantified the influenza transmission dynamics (e.g., attack rate, peak timing, and peak value) in northern and southern China from October 2022 to September 2023 (epidemiological year 2022–2023) using a mathematical compartmental model informed by influenza data from 2015 to 2019.

METHODS

We collected weekly influenza surveillance data from the Chinese National Influenza Center for northern and southern China from 2015 to 2023 (*15*). To map the influenza-like illness positive (ILI+) to the weekly symptomatic incidence of the general population, we optimized the health care seeking rate μ with a value from 0 to 1 with steps of 0.1; the least mean square error (MSE) of ILI+ was between the observation and mean estimates of 100 simulations of the fitting and forecast results for 2015–2019 and 2022–2023. The influenza season was defined following reference (ref.) (*16*).

We characterized influenza transmission in the population using a susceptible-symptomatic-asymptomatic-recovered-hospitalized-dead (SYARHD) model and used this model to simulate influenza transmission dynamics per season. To forecast influenza activity, we used the ensemble adjustment Kalman filter (EAKF) to infer the varying transmission coefficients in the mathematical transmission model following the parameter setting in ref. (*17*–*19*). We replayed the historical infection pattern with the inferred transmission rates to validate the effectiveness of model calibration. When simulating influenza activity in the future season, we set the transmission rates at time t as the average of the transmission rates at time t in the previous four influenza seasons (2015–2016, 2016–2017, 2017–2018, and 2018–2019). By doing so, we could simulate the influenza infection pattern for different situations (i.e., various proportions of the susceptible population). By using the distribution of (β_t) inferred by EAKF, we derived the 95% confidence interval (*CI*) of the number of new infections each week. Then, we aggregated the new infections in the whole flu season and calculated the attack rate as the proportion of the population that was infected.

RESULTS

According to the influenza surveillance data from the Chinese National Influenza Center (*15*), influenza activity continued to increase in February 2023 after the sudden relaxation of COVID-19 control measures; consequently, among the eight study years, the highest influenza activity was observed in 2023, followed by 2020, and the lowest activity was observed in 2021, with no apparent seasonality. In contrast to that in northern China, the influenza activity in southern China was more serious in the summer of 2022. In this period, the ILI+ and influenza-like illness (ILI) in southern China were 23.90 per 1,000 and 75.41 per 1,000 persons, respectively, which were higher than those in northern regions (4.44 per 1,000 and 27.77 per 1,000 persons, respectively). The ILI had a rebound increase in December 2022 and peaked at 130.96 per 1,000 and 86.25 per 1,000 persons in the southern and northern regions, respectively, during the Omicron variant outbreak in China, and resulted in notably increasing ILI cases compared with any other period. In February 2023, ILI+ had the highest values of 54.39 per 1,000 and 51.41 per 1,000 persons in the northern and southern regions, respectively.

To validate the epidemic models used in this study, we performed model calibration for influenza outbreaks in North and South China over five influenza seasons (2015–2016, 2016–2017, 2017–2018, 2018–2019, and 2022–2023). Informed by ILI+ (Figure 1), we used the EAKF algorithm (Methods) to infer the transmission rates in previous influenza seasons and replayed the historical infection pattern in the northern and southern regions of China (Figures 2–3).

We projected the influenza activity between October 9, 2022, and October 1, 2023 (Figure 4), with the transmission rate as the fitted value in the 2015–2019 seasons (Figure 3). During the study period, we estimated that the attack rates were 18.51% (95% *CI*: 0.00%, 37.78%) and 28.30% (95% *CI*: 14.77%, 41.82%) in northern and southern China, respectively. The influenza incidence was estimated to peak on March 12, 2023, and March 19, 2023, in northern and southern China, with ILI+ values of 61.28 (95%

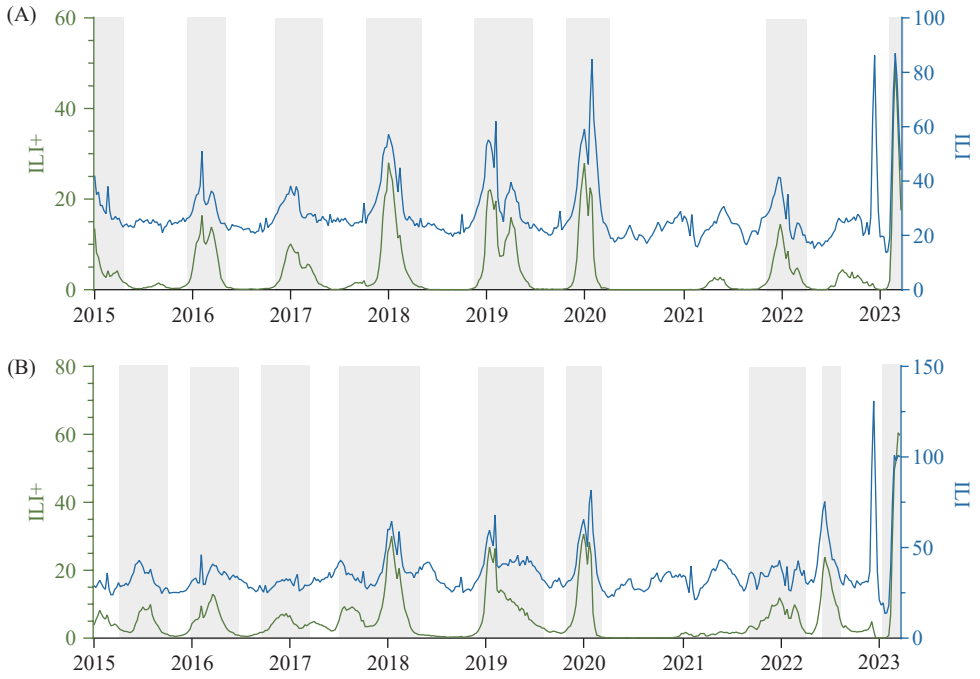

FIGURE 1. ILI and ILI+ in (A) northern China and (B) southern China.
Note: We estimated seasonal ILI+ (*20*) in northern and southern regions by multiplying the activities of ILI by public health laboratory estimates of percent positive influenza tests from the China CDC surveillance system for the 2015–2022 seasons. Gray shading represents the influenza seasons (*16*).
Abbreviation: ILI+=Influenza-like illness positive; ILI=Influenza-like illness.

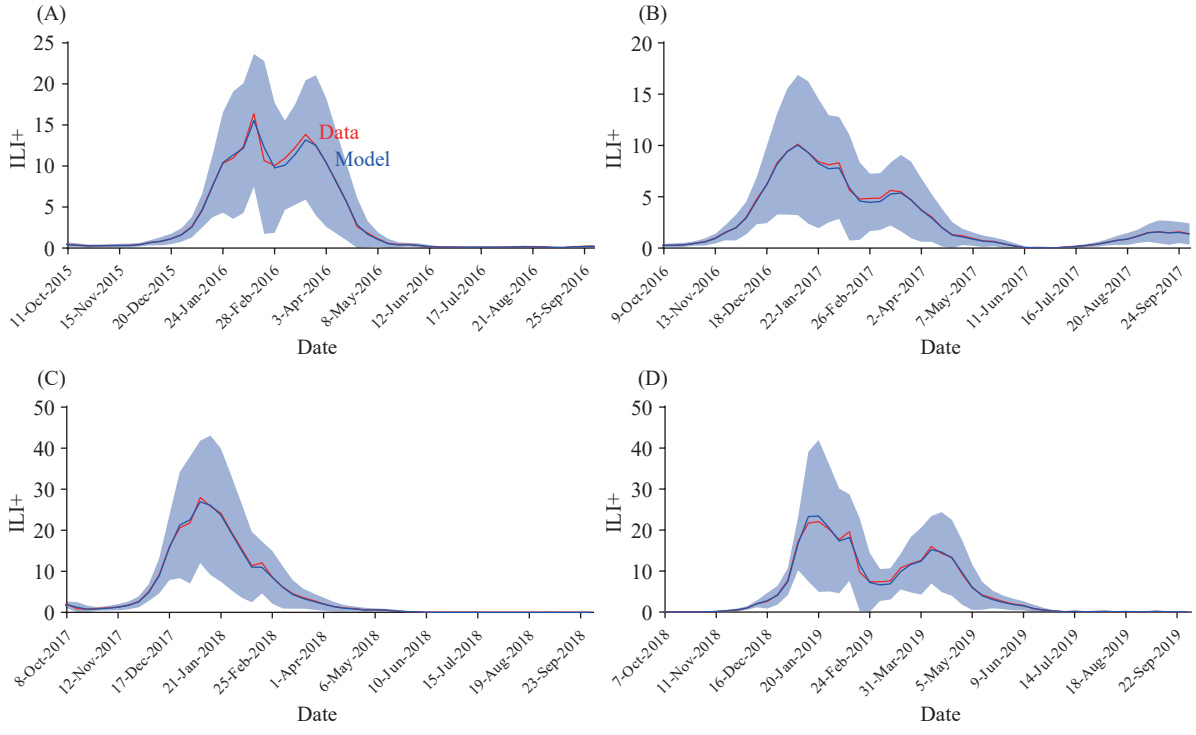

FIGURE 2. Reconstruction fit of ILI+ between 2015 and 2019 in northern regions. (A) 2015–2016; (B) 2016–2017; (C) 2017–2018; (D) 2018–2019.
Note: Blue lines and shaded areas indicate the mean and 95% *CI* of the estimation. The red line indicates the data.
Abbreviation: ILI+=Influenza-like illness positive; ILI=Influenza-like illness; *CI*=confidence interval.

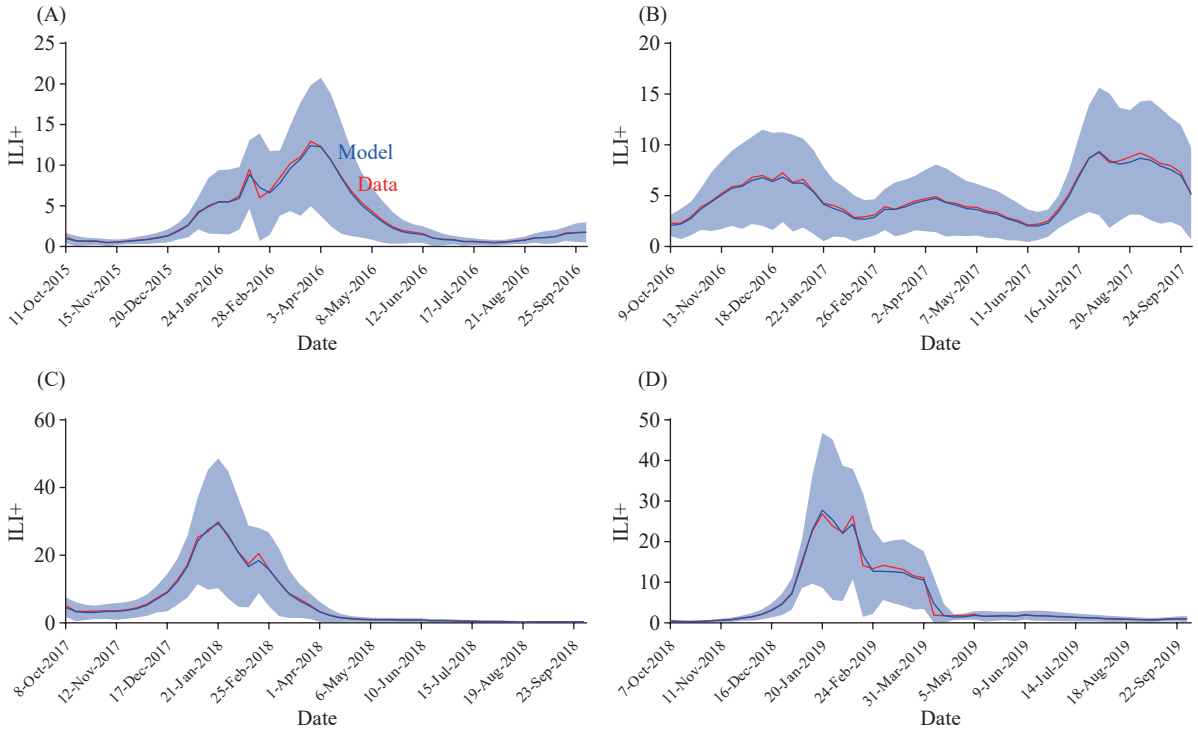

FIGURE 3. Reconstruction of ILI+ between 2015 and 2019 in southern regions. (A) 2015–2016; (B) 2016–2017; (C) 2017–2018; (D) 2018–2019.
Note: Blue lines and shaded areas indicate the mean and 95% *CI* of the estimation. The red line indicates the data.
Abbreviation: ILI+=Influenza-like illness positive; ILI=Influenza-like illness; *CI*=confidence interval.

CI: 0, 160.87) and 66.04 (95% *CI*: 0, 161.09), respectively, and the outbreaks were predicted to end on June 18 and July 23, 2023, in northern and southern China, respectively. For the influenza season of 2022–2023, the attack rate was estimated to exceed 5% in northern and southern China for 72% and 83% of the epidemics, respectively.

The effective reproduction number R_e between October 9, 2022, and October 1, 2023, started at 1.08 (95% *CI*: 0.51, 1.65) and 1.10 (95% *CI*: 0.55, 1.67) and reached as high as 2.13 (95% *CI*: 1.56, 2.70) on February 26, 2023, and 2.44 (95% *CI*: 1.86, 3.01) on February 26, 2023, while the mean estimates were 0.93 (95% *CI*: 0.35, 1.51) and 0.96 (95% *CI*: 0.44, 1.49), respectively, in northern and southern China. In contrast, the mean estimate was 0.97 (95% *CI*: 0.96, 0.98) and 0.99 (95% *CI*: 0.98, 1.00), with peak values of 1.60 (95% *CI*: 1.56, 1.65) and 1.42 (95% *CI*: 1.41, 1.43), for the period from October 2015 to September 2019 in northern and southern China, respectively.

The estimated proportions of the initially susceptible population (S_0) on October 9, 2022, were 0.73 and 0.76 in northern and southern China, respectively. Following the same R_e, a higher S_0 would cause both a higher ILI+ and attack rate. We further investigated the impact of susceptibility on the attack rate by varying S_0 from 50% to 80% across the transmission scenarios (Supplementary Figures S1–S2, available in https://weekly.chinacdc.cn/). In southern China, we estimated that the attack rates were 0.11% (95% *CI*: 0.04%, 0.19%), 0.45% (95% *CI*: 0%, 1.12%), 14.00% (95% *CI*: 3.37%, 24.62%), and 35.72% (95% *CI*: 18.21%, 53.24%) for S_0= 0.5, 0.6, 0.7, and 0.8, respectively. In northern China, we estimated that the attack rates were 0.18% (95% *CI*: 0.05%, 0.32%), 0.61% (95% *CI*: 0.00%, 1.26%), 10.27% (95% *CI*: 0.00%, 24.55%), and 42.54% (95% *CI*: 18.79%, 66.28%) for S_0= 0.5, 0.6, 0.7, and 0.8, respectively.

DISCUSSION

Infection with respiratory viruses, including influenza viruses and respiratory syncytial virus (RSV), typically occurs in seasonal patterns in China, with increased incidence during the cooler months of the year and around summer in southern China. However, due to the strict public health measures implemented during the COVID-19 pandemic, such as social distancing and wearing masks, the circulation of influenza was significantly reduced in 2020 and 2021.

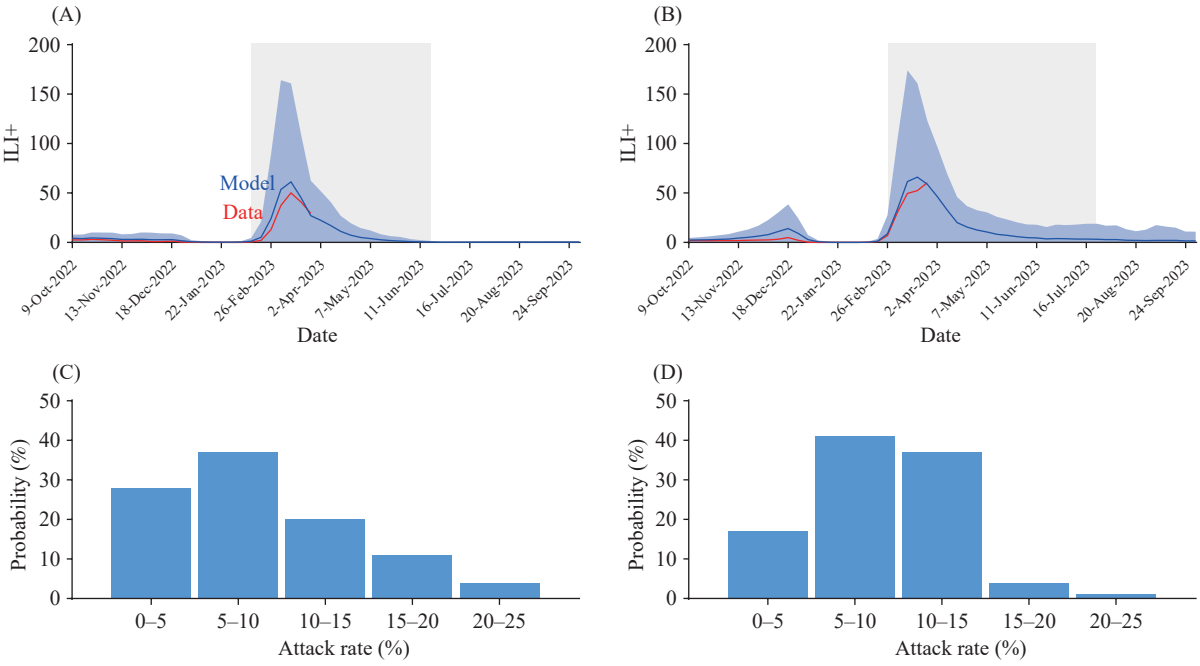

FIGURE 4. Projected ILI+ between October 9, 2022, and September 30, 2023. (A) The transmission rate in the 2022–2023 season in northern China, (B) the transmission rate in the 2022–2023 season in southern China; (C) probability distribution of the attack rate in northern China; (D) probability distribution of the attack rate in southern China.
Note: ILI+ is fitted before March 26, 2023, and projected after March 26 until September 30, 2023. We used the mean estimates of the four fitted transmission rates per week for the 2015–2016, 2016–2017, 2017–2018, and 2018–2019 seasons as the transmission rate for the same week in the 2022–2023 season. We ran 100 stochastic simulations and estimated the weekly incidence. Blue lines and shaded areas indicate the mean and 95% *CI* of the model, whereas the red line denotes the observations. Gray shading represents the influenza season (*16*). We estimated the attack rate for the influenza season for each of the 100 stochastic simulations and estimated the probability distribution.
Abbreviation: ILI+=Influenza-like illness positive; ILI=Influenza-like illness; *CI*=confidence interval.

With the gradual relaxation of COVID-19 NPIs in late 2020 and further relaxation after the COVID-19 Omicron wave in late 2022, influenza started to spread in the community. It is important to remain vigilant and track influenza development when it circulates, especially among vulnerable populations such as older adults and those with underlying health conditions. Although considerable uncertainty exists regarding cocirculating influenza variants, vaccines, and NPIs, we projected that influenza activities peaked in March 2023 in northern and southern China.

Influenza epidemiology is characterized by seasonality, which is influenced by population contact patterns, viral survival, and host immunity (*21*). In temperate climate zones, influenza seasons are generally synchronized and occur during winter (*22*). However, pandemics can occur when a new influenza virus emerges and spreads globally, causing severe illness, death, and significant social and economic disruption. Some influenza pandemics have had unusual patterns of illness, with out-of-season waves reported. For example, during the 1918 pandemic, there were three waves of illness, with the first wave occurring in the spring of 1918, followed by a second, more severe wave in the fall of that year and a third wave in the winter and spring of 1919. The 2009 H1N1 pandemic also had an unusual pattern of illness, with a first wave occurring in the spring of 2009, followed by a larger second wave in the fall and winter of that year. These perturbations are typically limited to the first year of circulation of a pandemic virus (*22*).

Compared to previous influenza pandemics, recent influenza activity has been substantially disrupted by the COVID-19 pandemic. This pandemic has caused changes in contact patterns and mobility, which have affected the seasonal cycles of many infectious diseases globally, including influenza. When COVID-19 first emerged in 2020, there was little to no influenza activity in either hemisphere due to the reduction in human mobility and contact in response to COVID-19. However, influenza started to resurge in late 2021, with out-of-season activity in the Southern Hemisphere. A peak in weekly influenza cases was reported in Australia in June 2022, earlier than typical

and far exceeding the 5-year average (*23*). According to the March 20, 2023, World Health Organization update, influenza activity continued to decrease following the peak in late 2022 (*24*). In North America, most indicators of influenza activity were at end-of-season levels, while in Europe, overall influenza diagnoses decreased slightly, and influenza positivity rates decreased according to data from sentinel sites, although these values remained above the epidemic threshold at the regional level. In East Asia, the activity of influenza A (H1N1) pdm09, which was the predominant strain, steeply increased in China but decreased in the other reporting countries.

The rise in the prevalence of respiratory viruses may not solely be attributed to the relaxation of strict NPIs used during the pandemic and population behavioral changes in response to perceived levels of risk. Importantly, while COVID-19 has created many challenges, it has also highlighted the significance of maintaining good health and hygiene practices.

The influenza A (H1N1), A (H3N2) and B strains can cocirculate in an influenza season. According to the isolation and identification results for the influenza virus from the China CDC (*14*), nearly half of samples from infected individuals harbored B viruses between 2015 and 2019. However, more than 99% of virus-positive samples contained A viruses in 2023. Compared to influenza B, influenza A tends to be more transmissible (*25*) and more likely to cause a pandemic (*26*), which may have resulted in the higher peak in 2023 than before. In the summer of 2022, an H3N2 influenza outbreak occurred in southern regions and peaked on June 20, 2022, with an ILI+ of 23.9, while the maximum ILI+ in northern regions was only 4.44 for the same period. Although natural infection provides long-lived immunity (*27*) in southern regions, the estimated attack rate and S_0 in southern regions in 2022–2023 seasons are higher than that in northern regions.

For years, a global control strategy for influenza has been implemented based on regular vaccine strain updates, which are centered on the synchronicity of influenza circulation at the hemispheric level (*28*). The findings of this study have important practical implications for public health authorities. The return of influenza activity in 2021–2022 highlights the need for improved influenza vaccines and increased vaccination coverage. Public health authorities should prioritize the development and distribution of improved influenza vaccines and ensure that vaccination campaigns are widely promoted and accessible to all populations, particularly vulnerable groups such as older adults and those with underlying health conditions. Resource allocation should be carefully considered in the context of cocirculating influenza variants and the potential for pandemics. Public health authorities should prioritize the allocation of resources toward surveillance and early warning systems for influenza epidemics as well as the development and distribution of antiviral medications in addition to vaccine development and distribution. Given the limitations of this study, public health authorities should continue to monitor the situation closely and adjust their strategies accordingly. These strategies include ongoing surveillance of influenza activity, vaccine coverage and efficacy tracking, and evaluation of the impact of NPIs, such as social distancing and wearing masks, on influenza transmission.

The limitations of this study should be noted. Our model does not explicitly include contact patterns, mobility, vaccination or NPIs but captures these factors through our estimates of transmissibility. Second, we use weekly ILI+ and scaling factors to map ILI+ to the weekly symptomatic incidence of the general population from municipal-scale estimates to denote the transmission rate, which may bias the attack rate given the potential uncertainty in spatial heterogeneity.

CONCLUSION

Understanding influenza seasonality is important for predicting and preparing for future outbreaks. After the cancellation of COVID-19-related measures in China in December 2022, we expected that a significant increase in influenza activity would last for 4 months in northern and southern China starting from mid-February to mid-June 2023. Although pandemic influenza seasons can disrupt regular seasonal cycles, further research is needed to improve our understanding of influenza seasonality and the emergence of new viruses. This is a crucial time to initiate well-designed studies that can help us understand how seasonal factors, immunity, contact patterns, and infections interact.

Conflicts of interest: BJC has consulted for AstraZeneca, Fosun Pharma, GSK, Haleon, Moderna, Roche, and Sanofi Pasteur. The authors report no conflicts of interest.

Funding: Supported by grants from the AIR@InnoHK Programme of the Innovation and

Technology Commission of the Government of the Hong Kong Special Administrative Region and the Theme-based Research Scheme (T11-712/19-N) of the Research Grants Council of the Hong Kong SAR Government.

doi: 10.46234/ccdcw2023.206

[#] Corresponding author: Benjamin J. Cowling, bcowling@hku.hk.

[1] WHO Collaborating Center for Infectious Disease Epidemiology and Control, School of Public Health, LKS Faculty of Medicine, The University of Hong Kong, Hong Kong Special Administrative Region, China; [2] Laboratory of Data Discovery for Health Limited, Hong Kong Science and Technology Park, Hong Kong Special Administrative Region, China; [3] State Key Laboratory of Molecular Vaccinology and Molecular Diagnostics, School of Public Health, Xiamen University, Xiamen City, Fujian Province, China; [4] Department of Genetics, University of Cambridge, Cambridge, UK; [5] Institute for Health Transformation & School of Health & Social Development, Deakin University, Melbourne, Australia.

Submitted: July 16, 2023; Accepted: December 05, 2023

REFERENCES

1. Liu PC, Xu J. Resurgence of influenza virus activity during COVID-19 pandemic in Shanghai, China. J Infect 2023;86(1):66 – 117. http://dx.doi.org/10.1016/j.jinf.2022.09.025.
2. Huaxia. China Focus: China releases measures to optimize COVID-19 response. 2022. https://english.news.cn/20221111/d4399114a082438eaac32d08a02bf58d/c.html. [2023-2-4].
3. Huaxia. China Focus: COVID-19 response further optimized with 10 new measures. 2022. https://english.news.cn/20221207/ca014c043bf24728b8dcbc0198565fdf/c.html. [2023-2-4].
4. Lai SJ, Ruktanonchai NW, Zhou LC, Prosper O, Luo W, Floyd JR, et al. Effect of non-pharmaceutical interventions to contain COVID-19 in China. Nature 2020;585(7825):410 – 3. http://dx.doi.org/10.1038/s41586-020-2293-x.
5. University of Oxford. Coronavirus government response tracker. 2020. https://www.bsg.ox.ac.uk/research/research-projects/coronavirus-government-response-tracker. [2020-7-17].
6. Wang XT, Pasco RF, Du ZW, Petty M, Fox SJ, Galvani AP, et al. Impact of social distancing measures on coronavirus disease healthcare demand, Central Texas, USA. Emerg Infect Dis 2020;26(10):2361 – 9. http://dx.doi.org/10.3201/eid2610.201702.
7. Du ZW, Xu XK, Wang L, Fox SJ, Cowling BJ, Galvani AP, et al. Effects of proactive social distancing on COVID-19 outbreaks in 58 cities, China. Emerg Infect Dis 2020;26(9):2267 – 9. http://dx.doi.org/10.3201/eid2609.201932.
8. Feng LZ, Zhang T, Wang Q, Xie YR, Peng ZB, Zheng JD, et al. Impact of COVID-19 outbreaks and interventions on influenza in China and the United States. Nat Commun 2021;12(1):3249. http://dx.doi.org/10.1038/s41467-021-23440-1.
9. Cohen R, Ashman M, Taha MK, Varon E, Angoulvant F, Levy C, et al. Pediatric Infectious Disease Group (GPIP) position paper on the immune debt of the COVID-19 pandemic in childhood, how can we fill the immunity gap? Infect Dis Now 2021;51(5):418-23. http://dx.doi.org/10.1016/j.idnow.2021.05.004.
10. Ali ST, Lau YC, Shan SW, Ryu S, Du ZW, Wang L, et al. Prediction of upcoming global infection burden of influenza seasons after relaxation of public health and social measures during the COVID-19 pandemic: a modelling study. Lancet Glob Health 2022;10(11):e1612 – 22. http://dx.doi.org/10.1016/S2214-109X(22)00358-8.
11. Yang J, Atkins KE, Feng LZ, Pang MF, Zheng YM, Liu XX, et al. Seasonal influenza vaccination in China: landscape of diverse regional reimbursement policy, and budget impact analysis. Vaccine 2016;34(47):5724 – 35. http://dx.doi.org/10.1016/j.vaccine.2016.10.013.
12. Palache A, Rockman S, Taylor B, Akcay M, Billington JK, Barbosa P, et al. Vaccine complacency and dose distribution inequities limit the benefits of seasonal influenza vaccination, despite a positive trend in use. Vaccine 2021;39(41):6081 – 7. http://dx.doi.org/10.1016/j.vaccine.2021.08.097.
13. Zeng XX, Xie YR, Yang XK, Peng ZB, Tang J, Yang L, et al. SARS-CoV-2 surveillance through China influenza surveillance information system — China, December 1, 2022 to February 12, 2023. China CDC Wkly 2023;5(7):152 – 8. http://dx.doi.org/10.46234/ccdcw2023.027.
14. Chinese National Influenza Center. China influenza weekly report as of March 12, 2023. https://ivdc.chinacdc.cn/cnic/zyzx/lgzb/202303/t20230316_264314.htm. [2023-3-16]. (In Chinese).
15. Chinese National Influenza Center. Chinese national influenza center. https://ivdc.chinacdc.cn/cnic/en/Surveillance/. [2023-3-24].
16. Yang W, Cowling BJ, Lau EHY, Shaman J. Forecasting influenza epidemics in Hong Kong. PLoS Comput Biol 2015;11(7):e1004383. http://dx.doi.org/10.1371/journal.pcbi.1004383.
17. Pei S, Teng X, Lewis P, Shaman J. Optimizing respiratory virus surveillance networks using uncertainty propagation. Nat Commun 2021;12(1):222. http://dx.doi.org/10.1038/s41467-020-20399-3.
18. Du ZW, Fox SJ, Ingle T, Pignone MP, Meyers LA. Projecting the combined health care burden of seasonal influenza and COVID-19 in the 2020–2021 season. MDM Policy Pract 2022;7(1):23814683221084631. http://dx.doi.org/10.1177/23814683221084631.
19. Borchering RK, Gunning CE, Gokhale DV, Weedop KB, Saeidpour A, Brett TS, et al. Anomalous influenza seasonality in the United States and the emergence of novel influenza B viruses. Proc Natl Acad Sci USA 2021;118(5):e2012327118. http://dx.doi.org/10.1073/pnas.2012327118.
20. Wu P, Presanis AM, Bond HS, Lau EHY, Fang VJ, Cowling BJ. A joint analysis of influenza-associated hospitalizations and mortality in Hong Kong, 1998-2013. Sci Rep 2017;7(1):929. http://dx.doi.org/10.1038/s41598-017-01021-x.
21. Tamerius J, Nelson MI, Zhou SZ, Viboud C, Miller MA, Alonso WJ. Global influenza seasonality: reconciling patterns across temperate and tropical regions. Environ Health Perspect 2011;119(4):439 – 45. http://dx.doi.org/10.1289/ehp.1002383.
22. Lee SS, Viboud C, Petersen E. Understanding the rebound of influenza in the post COVID-19 pandemic period holds important clues for epidemiology and control. Int J Infect Dis 2022;122:1002 – 4. http://dx.doi.org/10.1016/j.ijid.2022.08.002.
23. Australian Government Department of Health and Aged Care. Influenza surveillance program. 2023. https://www.health.gov.au/our-work/influenza-surveillance-program?utm_source=health.gov.au&utm_medium=callout-auto-custom&utm_campaign=digital_transformation. [2023-3-22].
24. WHO. Global influenza programme. 2023. https://www.who.int/teams/global-influenza-programme/surveillance-and-monitoring/influenza-updates/current-influenza-update. [2023-3-22].
25. Dai HY, Zhou N, Chen MX, Li GQ, Yu X, Su Y, et al. Assess transmissibility of different influenza subtypes: based on a SEIABR model. Infect Genet Evol 2022;103:105319. http://dx.doi.org/10.1016/j.meegid.2022.105319.
26. CDC. Pandemic influenza. 2020. https://www.cdc.gov/flu/pandemic-resources/index.htm. [2023-3-23].
27. Krammer F. The human antibody response to influenza A virus infection and vaccination. Nat Rev Immunol 2019;19(6):383 – 97. http://dx.doi.org/10.1038/s41577-019-0143-6.
28. Saha S, Chadha M, Al Mamun A, Rahman M, Sturm-Ramirez K, Chittaganpitch M, et al. Influenza seasonality and vaccination timing in tropical and subtropical areas of southern and south-eastern Asia. Bull World Health Organ 2014;92(5):318 – 30. http://dx.doi.org/10.2471/BLT.13.124412.

SUPPLEMENTARY MATERIAL

Data

Weekly influenza surveillance data were obtained from the Chinese National Influenza Center (*1*) for northern and southern China from 2015 to 2023. The data reported each week included the number of influenza-like illness (ILI) cases at the sentinel hospitals and the number of positive cases of influenza A (H1N1, H3N2, and pdmH1) and influenza B (Yamagata and Victoria) that were examined in a laboratory. We calculated the weekly incidence rate of influenza by multiplying the ILI rate by the positive rate of viral detection.

The influenza season was defined in the following refference (*2*). The onset of influenza seasons refers to the first of three consecutive weeks when influenza-like illness positive (ILI+) records exceeded a prescribed baseline (40% quantile of the nonzero ILI+ records). The end of the season refers to the first of two consecutive weeks with ILI+ below the baseline following the onset of the season.

Since ILI+ was calculated according to the ILI and laboratory-positive rate, it only represents the influenza-positive proportion of the health care-seeking population. Therefore, in our study, we assumed a health care seeking rate μ to map ILI+ to the weekly symptomatic incidence of the general population and then to obtain the weekly incidence of the general population based on the weekly symptomatic incidence and the symptomatic proportion. For the optimal value of μ, we chose a value from 0 to 1 with steps of 0.1; the least mean square error (MSE) of ILI+ was between the observation and mean estimates of 100 simulations of the fitting and forecast results for 2015–2019 and 2022–2023.

Transmission Model

We characterized influenza transmission in the population using a susceptible-symptomatic-asymptomatic-recovered-hospitalized-dead (SYARHD) model and used this model to simulate influenza transmission dynamics per season. The model equations were as follows:

$$S_{t+1} = S_t - \beta_t \times S_t \times (Y_t + \omega \times A_t) + \gamma \times R_t \quad (1)$$

$$Y_{t+1} = Y_t + \sigma \times \beta_t \times S_t \times (Y_t + \omega \times A_t) - \alpha \times Y_t - \delta_2 \times Y_t \quad (2)$$

$$A_{t+1} = A_t + (1 - \sigma) \times \beta_t \times S_t \times (Y_t + \omega \times A_t) - \delta_1 \times A_t \quad (3)$$

$$R_{t+1} = R_4 + \delta_1 \times A_t + \delta_2 \times Y_t + \delta_3 \times H_t - \gamma \times R_t \quad (4)$$

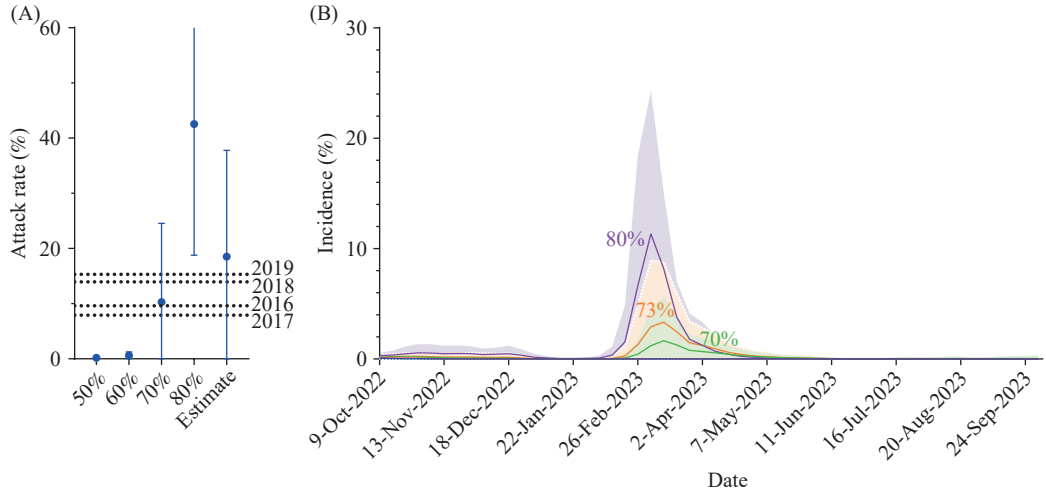

SUPPLEMENTARY FIGURE S1. Projected attack rates for the influenza outbreak in northern regions.
Note: Panel (A) is the estimated attack rates with the mean and 95% confidence interval (*CI*) between October 9, 2022, and September 30, 2023 across five transmission scenarios: 50%, 60%, 70%, 80% and our best estimate (73%) of the population initially susceptible on October 9, 2022. Panel (B) is the estimated incidence (%) of influenza infections across four scenarios. Black dotted horizontal lines correspond to attack rates for the same period during the 2015–2019 influenza seasons. We ran 100 stochastic simulations. Lines and shaded areas indicate the mean and 95% *CI* of the model.

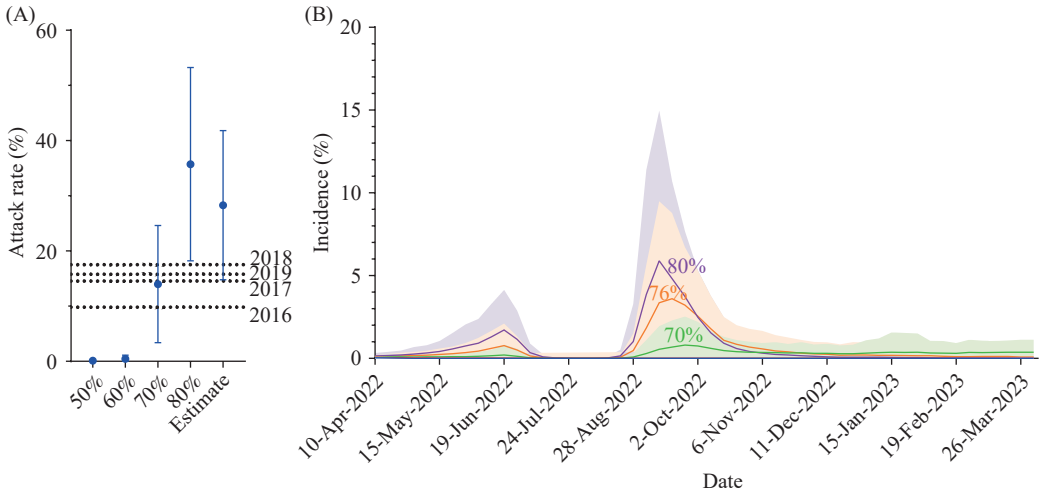

SUPPLEMENTARY FIGURE S2. Projected attack rates for the influenza outbreak in southern regions.
Note: Panel (A) estimated attack rates with the mean and 95% confidence interval (*CI*) between October 9, 2022, and September 30, 2023, across five transmission scenarios: 50%, 60%, 70%, 80% and our best estimate (78%) of the population initially susceptible on October 9, 2022. Panel (B) estimated incidence (%) of influenza infections across four scenarios. Black dotted horizontal lines correspond to attack rates for the same period during the 2015–2019 influenza seasons. We ran 100 stochastic simulations. Lines and shaded areas indicate the mean and 95% *CI* of the model.

$$H_{t+1} = H_t + \alpha \times Y_t - \delta_y \times H_t - \epsilon \times H_t \tag{5}$$

$$D_{t+1} = D_t + \epsilon \times H_t \tag{6}$$

Following infection at time t, susceptible individuals (S_t) enter an infectious state (symptomatic Y_t and asymptomatic A_t), in which a fraction of infected patients recover (R_t) at rate δ. Those recovered patients remain protected from future infection for the duration of $1/\gamma$ on average.

To forecast influenza activity, we used the ensemble adjustment Kalman filter (EAKF) to infer the varying transmission coefficient β_t at time t in the mathematical transmission model as well as the proportion of daily susceptible population S_t and infected population I_t and A_t. We set $\sigma = 0.55, \delta_1 = 1/3, \delta_2 = 1/5, \delta_3 = 0.9981$, $\alpha = 0.0146, \gamma = 1/(4 \times 365), \omega = 0.36$, and $\varepsilon = 0.0019$ following refs. (3–5). The effective reproduction number (R_e) at time t was calculated as follows:

$$R_t(t) = S_t \times \beta_t \times \left(\frac{\sigma}{\delta_2 + \alpha} + \omega \times \frac{1 - \sigma}{\delta_1} \right) \tag{7}$$

In each influenza season, we hierarchically inferred S_0 and β_t. For a given S_0, β_t was calibrated over time using EAKF. During the fitting period between 2015 and 2019, the initial S_0 values were drawn using latin hypercube sampling (LHS) from the range [0.65, 0.75] with 100 stochastic simulations (3). To forecast the influenza activity between October 9, 2022, and September 30, 2023, we chose a value from 0.65 to 1 with steps of 0.01; the least mean square error (MSE) of ILI+ was between the observation and mean estimates of 100 stochastic simulations.

In the parameter calibration of β_t, EAKF uses a group of particles (with population size N^p) to approximate the distribution of β_t. Specifically, one particle contains a specific combinatorial value of the hidden variables, for instance ($\beta^i{}_t$), and a group of particles are regarded as N^p random samples from the underlying distribution of these hidden variables (β_t). We set the number of particles N^p to 10,000.

To infer the hidden variables, EAKF assigns a weighting w_t to each particle according to its likelihood of generating the observed incidence. We model the influenza activity using the SIRS model on a daily basis, while the influenza incidence data are reported weekly. To align our model output with the reported data, we aggregate the daily new infection simulated by the SIRS model to weekly incidence, $dI_w = \sum_{t=d}^{d+6} \beta_t \times S_t \times (I_t + A_t)$, where d is the first day of week w. That is, we only calculate weightings for the end day of each week. The assigned weighting w_t is negatively proportional to the distance between the modeled weekly incidence and the observed ILI+ weekly incidence O_w, which we model using the Gaussian likelihood function: $w^i{}_t \propto \mathbb{N}\left(dI^i{}_w \middle| O_w, \Omega\right)$, where $\Omega = 0.25 \times O_w$. In the simulation of influenza activity at the next time step $t+1$, EAFK draws one particle from the particle group at

time step $t+1$ with probability $w^j{}_t, j \in [1, N^{\#}]$ and propagates to the next time step $t+1$ with the SIRS transmission model using the value of the drawn particle ($\beta^j{}_t$).

We replayed the historical infection pattern with the inferred transmission rates to validate the effectiveness of model calibration. When simulating the influenza activity in the future season, we set the transmission rates at time t as the average of the transmission rates at time t in the previous four influenza seasons (2015–2016, 2016–2017, 2017–2018, and 2018–2019). By doing so, we simulated the influenza infection pattern for different situations (i.e., various proportions of a susceptible population). By using the distribution of (β_t) inferred by EAKF, we derived the 95% confidence interval of the number of new infections each week. Then, we aggregated the new infections for the whole flu season and calculated the attack rate as the proportion of the population that was infected.

REFERENCES

1. Chinese National Influenza Center. Chinese national influenza center. https://ivdc.chinacdc.cn/cnic/en/Surveillance/. [2023-3-24].
2. Yang W, Cowling BJ, Lau EHY, Shaman J. Forecasting influenza epidemics in Hong Kong. PLoS Comput Biol 2015;11(7):e1004383. http://dx.doi.org/10.1371/journal.pcbi.1004383.
3. Pei S, Teng X, Lewis P, Shaman J. Optimizing respiratory virus surveillance networks using uncertainty propagation. Nat Commun 2021;12(1):222. http://dx.doi.org/10.1038/s41467-020-20399-3.
4. Du ZW, Fox SJ, Ingle T, Pignone MP, Meyers LA. Projecting the combined health care burden of seasonal influenza and COVID-19 in the 2020-2021 season. MDM Policy Pract 2022;7(1):23814683221084631. http://dx.doi.org/10.1177/23814683221084631.
5. Borchering RK, Gunning CE, Gokhale DV, Weedop KB, Saeidpour A, Brett TS, et al. Anomalous influenza seasonality in the United States and the emergence of novel influenza B viruses. Proc Natl Acad Sci USA 2021;118(5):e2012327118. http://dx.doi.org/10.1073/pnas.2012327118.